Guided subwavelength slow-light mode supported by a plasmonic waveguide system

Liu Yang,[1] Changjun Min,[2] and Georgios Veronis[1,2,*]

[1]*Department of Electrical and Computer Engineering, Louisiana State University, Baton Rouge, Louisiana 70803, USA*

[2]*Center for Computation and Technology, Louisiana State University, Baton Rouge, Louisiana 70803, USA*

**Corresponding author: gveronis@lsu.edu*

Received August 23, 2010; accepted November 13, 2010;
posted November 29, 2010 (Doc. ID 133786); published December 14, 2010

We introduce a plasmonic waveguide system, which supports a subwavelength broadband slow-light guided mode with a tunable slowdown factor at a given wavelength. The system consists of a metal–dielectric–metal (MDM) waveguide side-coupled to a periodic array of MDM stub resonators. The slowdown factor at a given wavelength can be tuned by adjusting the geometrical parameters of the system. In addition, there is a trade-off between the slowdown factor and the propagation length of the supported optical mode. Finally, we show that light can be coupled efficiently from a conventional MDM waveguide to the plasmonic waveguide system.

OCIS codes: 240.6680, 230.7370, 130.2790.

Plasmonic waveguides, based on surface plasmons propagating at metal–dielectric interfaces, have shown the potential to guide and manipulate light at deep subwavelength scales, and could provide an interface between conventional optics and subwavelength electronic and optoelectronic devices [1,2]. In addition, slowing down light in plasmonic waveguides leads to enhanced light–matter interaction, and could, therefore, enhance the performance of nanoscale plasmonic devices, such as switches and sensors [3–8]. Several different nanoscale plasmonic waveguiding structures have been recently proposed, such as metallic nanowires, metallic nanoparticle arrays, V-shaped grooves, and metal–dielectric–metal (MDM) waveguides [9]. Among these, MDM plasmonic waveguides, which are the optical analogue of microwave two-conductor transmission lines [10], are of particular interest because they support modes with deep subwavelength scale over a very wide range of frequencies extending from DC to visible [11]. However, in conventional MDM plasmonic waveguides, once the operating wavelength and modal size are fixed, the group velocity of light is not tunable.

In this Letter, we introduce a plasmonic waveguide system, which supports a subwavelength broadband slow-light guided mode with a tunable slowdown factor at a given wavelength. The structure is a plasmonic analog of the periodically loaded transmission lines used in microwave engineering [10]. We show that the principle of operation of such a system can be explained using a characteristic impedance model and transmission line theory. We find that the slowdown factor at a given wavelength can be tuned by adjusting the geometrical parameters of the system. We also find that there is a trade-off between the slowdown factor and the propagation length of the supported optical mode. Finally, we show that light can be coupled efficiently from a conventional MDM waveguide to the plasmonic waveguide system. Such slow-light plasmonic waveguide systems could be potentially used in nonlinear, switching, and sensing applications.

The structure consists of an MDM waveguide side-coupled to a periodic array of MDM stub resonators [Fig. 1(a)]. Side-coupled-cavity structures have been previously proposed as compact filters, reflectors, switches, and impedance matching elements for plasmonic waveguides [12–15]. Both the MDM waveguide and MDM stub resonators have deep subwavelength widths ($w_0, w \ll \lambda$). The periodicity d is also subwavelength ($d \ll \lambda$), so that the operating wavelength is far from the Bragg wavelength of the waveguide [16] ($\lambda \gg \lambda_{\mathrm{Bragg}}$). In addition, the distance between adjacent side-coupled cavities d–w is chosen large enough so that direct coupling between the cavities has a negligible effect on the dispersion relation of the system. This sets a lower limit on the periodicity $d_{\min}$ of the plasmonic waveguide structure. For $w = 50\,\mathrm{nm}$, we found that $d_{\min} \simeq 80\,\mathrm{nm}$.

We use a finite-difference frequency-domain (FDFD) method [17] to investigate the properties of the structure. This method allows us to directly use experimental data for the frequency-dependent dielectric constant of metals, such as silver [18], including both the real and imaginary parts, with no approximation. Perfectly matched layer (PML) absorbing boundary conditions are used at all boundaries of the simulation domain [19]. To drastically reduce spurious reflections at PML interfaces, we place ~20 periods of the waveguiding structure within the PML layer [20].

We use a characteristic impedance model and transmission line theory [15,21] to account for the behavior of the system. Based on transmission line theory, the system is equivalent to a transmission line with characteristic impedance $Z_0 = \gamma_0 w_0/(i\omega\varepsilon)$ periodically loaded with short-circuited transmission line stub resonators of length L and characteristic impedance $Z_1 = \gamma_1 w/(i\omega\varepsilon)$. Here, γ_0 (γ_1) is the complex wave vector of the fundamental propagating TM mode in a MDM waveguide of width w_0 (w) [Fig. 1(a)]. Using transmission line theory [10], the dispersion relation between ω and the Bloch wave vector $\gamma = \alpha + i\beta$ of the entire system is found to be

$$\cosh(\gamma d) = \cosh^2\left(\gamma_0 \frac{d}{2}\right) + \sinh^2\left(\gamma_0 \frac{d}{2}\right) + \frac{Z_1}{Z_0} \sinh\left(\gamma_0 \frac{d}{2}\right) \cosh\left(\gamma_0 \frac{d}{2}\right) \tanh(\gamma_1 L). \quad (1)$$

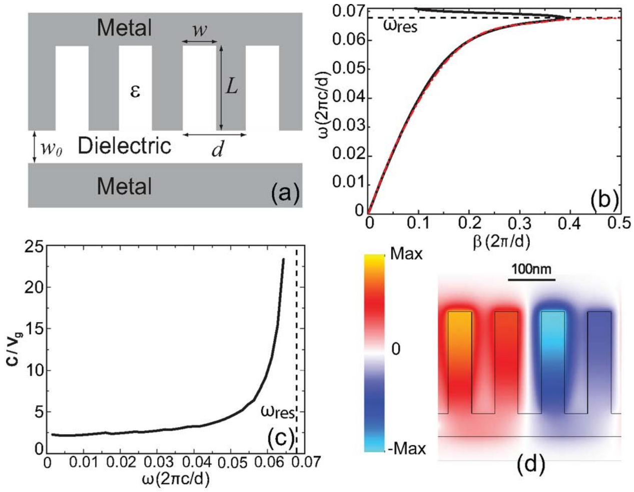

Fig. 1. (Color online) (a) Schematic of a plasmonic waveguide system consisting of a MDM waveguide side-coupled to a periodic array of MDM stub resonators. (b) Dispersion relation of the plasmonic waveguide system of Fig. 1(a) calculated using FDFD (black solid curve). Results are shown for a silver–air structure with $d = 100\,\text{nm}$, $L = 220\,\text{nm}$, and $w_0 = w = 50\,\text{nm}$. Also shown is the dispersion relation for lossless metal (red dashed–dotted line), and the resonance frequency ω_{res} (black dashed line) ($\omega_{\text{res}} \simeq 0.067 \cdot 2\pi c/d$ corresponding to $\lambda_{\text{res}} \simeq 1.5\,\mu\text{m}$). (c) Reciprocal of the group velocity v_g of light in the plasmonic waveguide system as a function of frequency. All parameters are as in Fig. 1(b). (d) Magnetic field profile of the supported optical mode in the system at $\lambda_0 = 1.55\,\mu\text{m}$. All other parameters are as in Fig. 1(b).

In Fig. 1(b), we show the dispersion relation for the plasmonic waveguiding structure of Fig. 1(a) calculated using FDFD, which, similar to surface plasmons propagating at a single metal–dielectric interface [16], exhibits a resonance. In the lossless metal case, the resonance frequency ω_{res} is the cutoff frequency of the fundamental mode, and, for $\omega > \omega_{\text{res}}$, the system has a bandgap, supporting a nonpropagating mode with $\beta = 0$. In addition, we have $\gamma_0 = i\beta_0$, $\gamma_1 = i\beta_1$, and $\beta(\omega_{\text{res}}) = \pi/d$ at the band edge. Using these and Eq. (1), we find that the resonance frequency ω_{res} is a solution of the following equation:

$$Z_1(\omega_{\text{res}}) \tan[\beta_1(\omega_{\text{res}})L] = 2Z_0(\omega_{\text{res}}) \cot\left[\beta_0(\omega_{\text{res}})\frac{d}{2}\right]. \quad (2)$$

Thus, unlike in conventional MDM waveguides, where ω_{res} is equal to the surface plasmon frequency of the metal–dielectric interface ($\omega_{\text{res}} = \omega_{\text{sp}}$) and is fixed for a given metal [16], in such a plasmonic waveguide system the resonance frequency ω_{res} is tunable through its geometric parameters. In the presence of loss, we have $\beta(\omega_{\text{res}}) < \pi/d$ [Fig. 1(b)]. In addition, for $\omega > \omega_{\text{res}}$ the Bloch wave vector γ has an imaginary component ($\beta \neq 0$), and the dispersion relation experiences back-bending [16] with negative group velocity $v_g \equiv \frac{\partial\omega}{\partial\beta}$ [Fig. 1(b)].

In such a plasmonic waveguide system, light is slowed down over a very wide frequency range extending from DC to slightly below the resonance frequency [Fig. 1(c)]. To find the slowdown factor c/v_g in the low-frequency limit, we take the limit of the dispersion relation in Eq. (1) as $\omega \to 0$. We note that, in the limit of $\omega \to 0$, $\gamma_0 \simeq \gamma_1 \simeq i\omega\sqrt{\varepsilon\mu_0}$. Using these, we obtain the low-frequency ($\omega \to 0$) slowdown factor $c/v_g = \sqrt{1 + \frac{wL}{w_0 d}}$. We confirmed that this analytical result is in excellent agreement with the result obtained using FDFD. Thus, the group velocity of the system in the low-frequency regime is entirely controlled by its geometry. When ω approaches ω_{res} ($\omega \lesssim \omega_{\text{res}}$), the dispersion relation becomes flat, and the group velocity v_g rapidly decreases [Fig. 1(c)].

We found that, at frequencies far from the resonance frequency, the modal energy of the periodic plasmonic waveguide extends over both the waveguide and the stub resonators. On the other hand, at frequencies near the resonance frequency, the field intensity in the resonators is enhanced, and the modal energy is, therefore, mostly concentrated in the resonators [Fig. 1(d)]. In both cases, the modal size is subwavelength.

The slowdown factor in the system at a given wavelength can be tuned by adjusting the geometric parameters of the structure. In Fig. 2(a), we show the slowdown factor c/v_g as a function of the stub length L at $\lambda_0 = 1.55\,\mu\text{m}$. For $L = 0$, the structure is a conventional MDM waveguide and $\omega_{\text{res}} = \omega_{\text{sp}}$. Since the operating frequency ω is far from the resonance frequency of the system ω_{res}, the slowdown factor is small [Fig. 1(c)]. As L increases, ω_{res} decreases [Eq. (2)] and, because the operating frequency approaches the resonance frequency, the slowdown factor increases [Fig. 2(a)]. Thus, by adjusting the stub length L, the group velocity of the mode can be tuned to a desired value at the operating wavelength.

In Fig. 2(a), we also show the slowdown factor c/v_g calculated by transmission line theory. We observe that there is very good agreement between the transmission line theory results and the exact results obtained using FDFD. We note that the small difference between the transmission line theory and FDFD results is due to the error introduced by the transmission line model in the phase of the reflection coefficient at the two interfaces of the side-coupled cavity of length L. Such limitations of the characteristic impedance model for circuits of MDM plasmonic waveguides have been described in detail elsewhere [22].

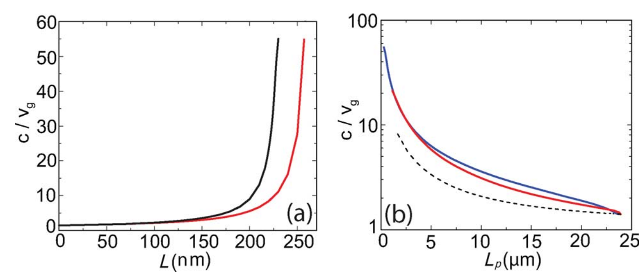

Fig. 2. (Color online) (a) Reciprocal of v_g as a function of L for the plasmonic waveguide system of Fig. 1(a) at $\lambda_0 = 1.55\,\mu\text{m}$ calculated using FDFD (left black curve) and transmission line theory (right red curve). All other parameters are as in Fig. 1(b). (b) Reciprocal of v_g versus propagation length L_p for the plasmonic waveguide system of Fig. 1(a) at $\lambda_0 = 1.55\,\mu\text{m}$ calculated using FDFD. Results are shown for $d = 100\,\text{nm}$ (upper blue curve) and $d = 200\,\text{nm}$ (lower red curve) as L is varied. All other parameters are as in Fig. 1(b). We also show c/v_g versus L_p for a conventional MDM waveguide at $\lambda_0 = 1.55\,\mu\text{m}$ (dashed curve) as the width of its dielectric region is varied.

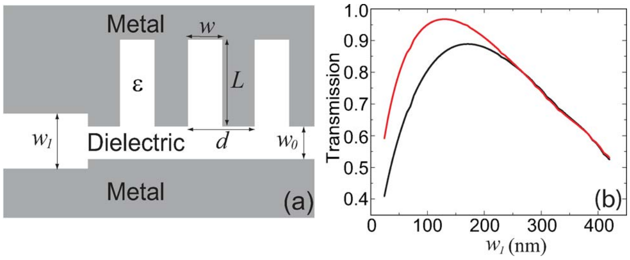

Fig. 3. (Color online) (a) Schematic of a coupler between a conventional MDM waveguide and the plasmonic waveguide system of Fig. 1(a). (b) Transmission for the coupler of Fig. 3(a) as a function of w_1 for $L = 190$ nm (upper red curve), and for $L = 220$ nm (lower black curve) calculated using FDFD. All other parameters are as in Fig. 1(b).

In addition, due to the absorption loss in the metal, there is a trade-off between the slowdown factor c/v_g and the propagation length L_p of the supported optical mode in such slow-light plasmonic waveguide systems [Fig. 2(b)]. For a given slowdown factor, the mode of the plasmonic waveguide system has a significantly larger propagation length when compared to a conventional MDM plasmonic waveguide [Fig. 2(b)]. This is because, in a conventional MDM waveguide, the slowdown factor can be increased by decreasing the dielectric layer width. This, however, also results in increase of the fraction of the modal power in the metal.

We finally consider the coupling between the plasmonic waveguide system [Fig. 1(a)] and a conventional MDM waveguide. To achieve high transmission efficiency, the characteristic impedance of the input MDM waveguide must be matched to the characteristic impedance of the system [21]. We note that the characteristic impedance of an MDM waveguide can be tuned by adjusting its width [21]. Thus, by simply placing the MDM waveguide terminated flat at the entrance of the plasmonic waveguide system and adjusting its width w_1 [Fig. 3(a)], we can achieve almost perfect impedance matching between the two waveguiding structures, and, therefore, very high transmission efficiency [Fig. 3(b)]. We also note that the transmission can be even further improved by using a single intermediate MDM waveguide section between the two structures. Thus, no adiabatic tapering structures are required to couple light efficiently into the plasmonic waveguide system. This enables the use of the system in highly compact plasmonic devices for enhanced light-matter interaction.

This research was supported by the Louisiana Board of Regents (contracts LEQSF(2009-12)-RD-A-08 and NSF (2010)-PFUND-187).

References

1. W. L. Barnes, A. Dereux, and T. W. Ebbesen, Nature **424**, 824 (2003).
2. E. Ozbay, Science **311**, 189 (2006).
3. A. Karalis, E. Lidorikis, M. Ibanescu, J. Joannopoulos, and M. Soljacic, Phys. Rev. Lett. **95**, 063901 (2005).
4. M. Sandtke and L. Kuipers, Nat. Photon. **1**, 573 (2007).
5. Z. Kang, W. Lin, and G. P. Wang, J. Opt. Soc. Am. B **26**, 1944 (2009).
6. Q. Gan, Y. J. Ding, and F. J. Bartoli, Phys. Rev. Lett. **102**, 056801 (2009).
7. A. Kocabas, S. S. Senlik, and A. Aydinli, Phys. Rev. Lett. **102**, 063901 (2009).
8. E. Feigenbaum and M. Orenstein, Opt. Express **17**, 2465 (2009).
9. D. K. Gramotnev and S. I. Bozhevolnyi, Nat. Photon. **4**, 83 (2010).
10. D. M. Pozar, *Microwave Engineering* (Wiley, 1998).
11. E. N. Economou, Phys. Rev. **182**, 539 (1969).
12. Y. Matsuzaki, T. Okamoto, M. Haraguchi, M. Fukui, and M. Nakagaki, Opt. Express **16**, 16314 (2008).
13. X. S. Lin and X. G. Huang, Opt. Lett. **33**, 2874 (2008).
14. J. Liu, G. Fang, H. Zhao, Y. Zhang, and S. Liu, Opt. Express **17**, 20134 (2009).
15. C. Min and G. Veronis, Opt. Express **17**, 10757 (2009).
16. S. A. Maier, *Plasmonics: Fundamentals and Applications* (Springer, 2007).
17. S. D. Wu and E. N. Glytsis, J. Opt. Soc. Am. A **19**, 2018 (2002).
18. E. D. Palik, *Handbook of Optical Constants of Solids* (Academic, 1985).
19. J. Jin, *The Finite Element Method in Electromagnetics* (Wiley, 2002).
20. M. Koshiba, Y. Tsuji, and S. Sasaki, IEEE Microw. Wirel. Compon. Lett. **11**, 152 (2001).
21. G. Veronis and S. Fan, Appl. Phys. Lett. **87**, 131102 (2005).
22. S. E. Kocabas, G. Veronis, D. A. B. Miller, and S. Fan, IEEE J. Sel. Top. Quantum Electron. **14**, 1462 (2008).